



AgEcon SEARCH
RESEARCH IN AGRICULTURAL & APPLIED ECONOMICS

The World's Largest Open Access Agricultural & Applied Economics Digital Library

This document is discoverable and free to researchers across the globe due to the work of AgEcon Search.

Help ensure our sustainability.

Give to AgEcon Search

AgEcon Search

<http://ageconsearch.umn.edu>

aesearch@umn.edu

*Papers downloaded from **AgEcon Search** may be used for non-commercial purposes and personal study only. No other use, including posting to another Internet site, is permitted without permission from the copyright owner (not AgEcon Search), or as allowed under the provisions of Fair Use, U.S. Copyright Act, Title 17 U.S.C.*

No endorsement of AgEcon Search or its fundraising activities by the author(s) of the following work or their employer(s) is intended or implied.



Geostatistical Assessment of Forest-Based, Exponential Smoothing and Curve Fitting Algorithms in Forecasting Wet and Dry Conditions of the Short Rain Season at a Local Scale in Uganda

Ivan Bamweyana¹, Moses Musinguzi¹, Lydia Mazzi Kayondo¹

¹Department of
Geomatics and
Land Management,
Makerere
University,
Kampala, Uganda
Email:
ivanson5@gmail
l.com

Abstract

Context and objectives:

Climate extremes associated with wet and dry conditions are one of the main causal elements of the disasters that adversely impact Uganda's agriculturally based economy. However, the lack of reliable forecast records for wet and dry conditions remains a challenge at a local scale. Given the proliferation of geostatistical forecast algorithms, this study assessed the suitability of three forecast algorithms: forest-based, exponential smoothing and curve fitting in forecasting wet and dry conditions at a local scale in Uganda.

Methodology:

The CHIRPS satellite gridded datasets for the variable short rains season of September, October, and November (SON) for the 1981-2020 historical period were used to develop the forecasts and the 2021-2022 period was used to validate the forecasts. The Standardized Precipitation Index (SPI) derived from the CHIRPS dataset was used as the proxy for wet and dry conditions. The three algorithms were assessed by subjecting them to the SPI space-time cube structure in the ArcGIS environment. Using the resultant Forecast and Validation Root Mean Square Error (FRMSE and VRSME respectively), forecast models were then generated for each of the algorithms. A comparison of the least VRSME at every locality from any of the three algorithms was then used to build a joint forecast model.

Results:

Results from the three algorithms demonstrate that each locality experiences an independent forecast regardless of the influence of the immediate neighbourhood, and by 2025, the majority of the localities will experience moderately wet conditions during the SON season. The forest-based forecast, exponential smoothing, curve fitting and the combined least VRMSE forecast produced a best value of $R^2=0.33, 0.48, 0.4$ and 0.62 respectively upon validation of the exact value. However, for values within the 95% confidence interval band, an $R^2 =0.89, 0.83$ was realized for the forest-based and exponential smoothing. Based on the behavioural performance of the algorithms, results further reveal that most of the localities in the study area exhibit complex patterns and can best be predicted by forest-based algorithms. The results from this study support the motive of the Sustainable Development Goal (SDG) 13 by enabling the communication of empirical studies on locally determined climate contributions. The knowledge gained regarding localized wet and dry conditions prediction will help to increase the capacity of local governance and decision-making organizations that adopt and put into practice local disaster risk reduction initiatives. Further research is needed to assess the driving factors behind the pattern behaviours at the different localities

Keywords: Wet and Dry Conditions, Geostatistics, Forecasting, Precipitation, Local scale

1 Introduction

Of the disasters that affect localities in Uganda, 70% are climate-related. These disasters have been reported to destroy an average of 800,000 hectares of crops leading to an economic loss above 120 billion Uganda shillings (US \$32.4 million) annually (Mugenyi et al., 2011). To combat this, the Ugandan government is frantically pursuing policies that will shift the disaster management paradigm from the conventional emergency response focus to one of preparedness based on scientific forecasts at a local scale (Bamweyana & Kayondo, 2017). This creates an urgent and critical requirement, therefore, to develop and incorporate local spatial forecasts into the climate-sensitive policy development process at a local scale. The primary climate factor currently contributing to these disasters is precipitation. Understanding, therefore, the spatial variability and forecast of wet and dry conditions associated with precipitation is critical to improving the degree of choice under which local climate policy is developed (Bartholy & Pongracz, 2004; Duhan & Pandey, 2013).

A big part of Uganda experiences a bimodal rainfall pattern consisting of two rainy seasons (Nsubuga & Rautenbach, 2018), with the first annual rains also called the long rains occurring roughly in March, April, and May (MAM). The second rains occur around September, October, and November (SON) and are called short rains. Of the two rainy seasons, the SON short rains show substantial inter-annual variability with greater impacts on wet and dry conditions (Kolstad & MacLeod, 2022). Notably, there is also a lack of scientific consensus on the seasonal and spatial forecast of rainfall experienced in Uganda in and around the SON season (Osbahe et al., 2011). Hepworth & Goulden, (2008) indicate that there is a chance that the mean annual rainfall would rise significantly after 2060, with less certainty. The biggest percentage increase in rainfall is predicted to occur in December, January, and February (DJF). This could make the short rains of SON longer (Atube et al., 2022). Similarly, Chris et al., (2012) spatially observe that given the current trends, the bimodal areas across the country are likely to experience an increase in SON rainfall in the period between 2010 and 2039. On the contrary, Mubiru et al., (2018); Nandozi et al., (2012) urge that with Regional Climate Models (RCM), the SON is likely to experience a downward trend at 0.7 mm day^{-1} . Other related research has argued that there is no significant change in the average rainfall both for the past 60-year record and the period between 2015-2045 (MWLE, GEF, (2002); USAID, (2013)). All these studies, however, have general concusses about the increase in the intensity and frequency of wet and dry conditions associated with precipitation. Unfortunately, these studies generalize at a national level and are silent on the spatial forecast at a local scale. Several geostatistical approaches exist (Kleiber et al., 2011; Res et al., 2003) and are widely used in applied fields to forecast data (Arbia & Di Marcantonio, 2015) including precipitation forecast (Anshuka et al., 2022). With the proliferation of data cubes as 3D schemas optimized for spatial time series analysis (Purwanto et al., 2021), dominant geostatistical algorithms of location-based forecast have emerged. However, in the forecasting of wet and dry conditions at a local scale in Uganda, the suitability of some of these algorithms has not been assessed. This research, therefore, seeks to carry out a geostatistical suitability assessment of forest-based, exponential smoothing and curve fitting forecast algorithms in forecasting wet and dry conditions in the SON (short rains) season in Uganda. The ability to spatially forecast the variability of the wet and dry conditions at a local scale has a positive bearing on the country's overall development given the predominance of rain-fed agriculture (Bigirimana, 2012) that is majorly influenced by local occurrence of rainfall.

2 Study area, Data and Materials

2.1 Study Area

Uganda is a landlocked country in the eastern part of Africa. Being crossed by the equator, the country lies greatly within the northern hemisphere and partly in the southern hemisphere. The neighbouring countries are South Sudan to the North, Kenya to the East, the United Republic of Tanzania and Rwanda to the South and the Democratic Republic of Congo to the West. According to Bamweyana et al., (2021) and SNC, (2014), the country has a total surface area of 241,550 km² of which 41,743 km² (17.2 %) is occupied by open water and swamps, and 199,807 km² is open land. At a mesoscale, the country is mostly surrounded by significant physical features including the Lake Victoria basin, mountain ranges, and the vast Congo Basin forest to the west that affect the spatial-temporal distribution of precipitation intensity and variability. The map in Figure 1 shows the location of Uganda in Africa, its administrative districts and large water bodies.

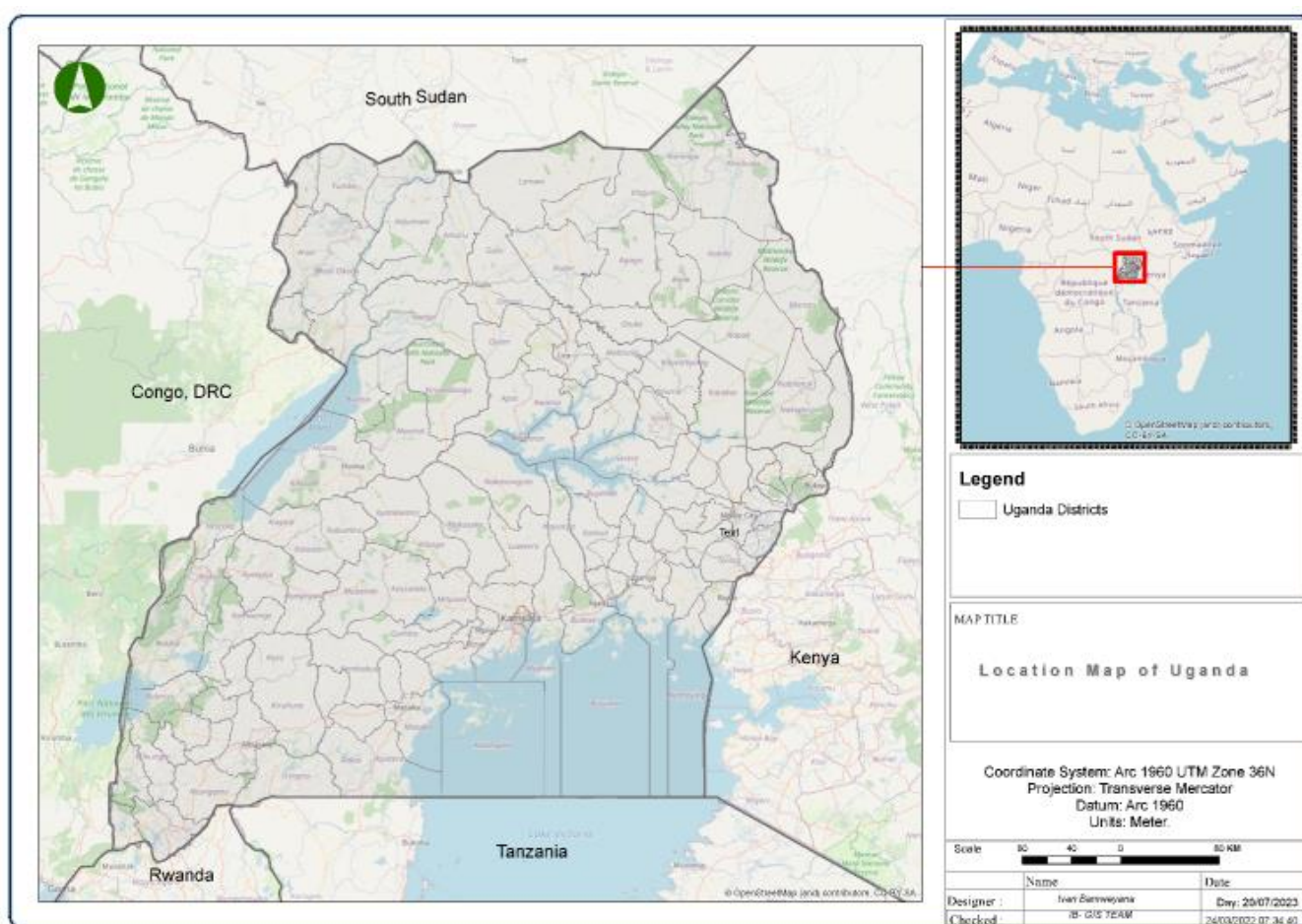


Figure 1: Location Map of Uganda

2.2 Data and Materials

Uganda is characterized by a critically sparse and unreliable rain gauge network (Bamweyana et al., 2021). This study, therefore, adopted the satellite-gridded datasets as the alternative rainfall estimate. Throughout the literature, several gridded datasets have been evaluated as alternative rainfall estimates (Bamweyana et al., 2021; Dinku et al., 2018). Based on these evaluations, the CHIRPS satellite gridded dataset has emerged as the better estimate for precipitation in Uganda and East Africa and has been adopted by several researchers (Bamweyana & Kayondo, 2017; Diem et al.,

2014; Muthoni et al., 2019; Ngoma et al., 2021). Similarly, this study utilised the CHIRPS as the Satellite-based Precipitation Estimator (SPE). The CHIRPS gridded rainfall data (Funk et al., 2015) blends station precipitation data with infrared Cold Cloud Duration (CCD) at $0.05^\circ * 0.05^\circ$ (latitude, longitude) spatial resolution to produce a satellite-gridded dataset from 1981 to date.

3 Methods

In various studies, the SPI datasets, which are derived from satellite-gridded datasets, have been utilized as a proxy for wet and dry conditions. (Ford et al., 2021; Khandu et al., 2016; Long et al., 2012; Wang et al., 2017). The World Meteorological Organization (WMO) assesses SPI -3 as a more effective proxy for wet and dry conditions especially in highlighting moisture conditions than other hydrological indices (Svoboda et al., 2012). In the monthly computation of SPI-3 of a given year say; 2006, a three (3) months precipitation total for the precipitation season SON in 2006 was compared to the SON precipitation totals of all the years on record (1981-2020). This reflected short and medium-term moisture conditions while providing a seasonal estimation of precipitation. A time-structured gridded dataset for the SON season was then re-structured into a spatial abstraction dataset for storing and retrieving multidimensional data format called Network Common Data Form (NetCDF) (Fouilloux, 2022). This was represented by a space-time cube which is a three-dimensional (3D) cube that consists of space-time bins (x, y, t) in which the x and y dimensions are raster cell squares that represent localities within the cube (spatial extent). The t dimension represents time in a one-year increment (temporal extent) as represented in the grid cube shown in Figure 2. This structuring enabled integrated spatial and temporal analysis per location/locality in the study area. The location accounts for the local scale.

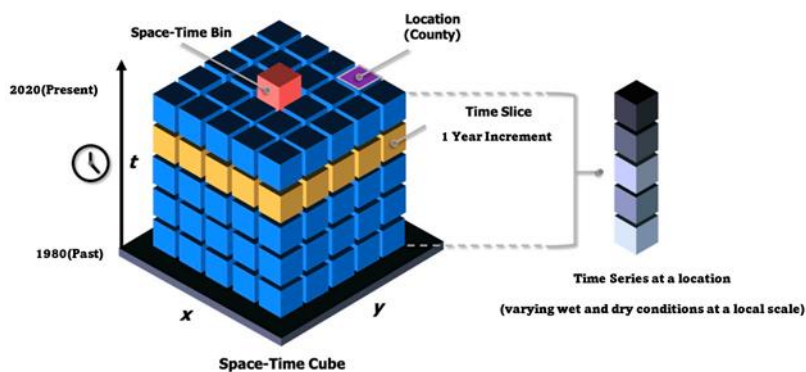


Figure 2: Structure of the space-time cube. Modified from Park et al., (2021)

3.1 Location Based forecasting

The data cube was then subjected to location-based forecasting. In this approach, we employed three location forecasting algorithms. That is curve-fitting, exponential smoothing, and forest-based forecasting. However, for each of these algorithms to make a forecast at a given location of the space-time data cube, two underlying models were used to forecast the time series.

3.1.1 The forecast model

The forecast model was used to forecast values at each time step of a location. It was constructed by fitting a given curve type under a given algorithm to the time series at each of the locations in the

space-time cube. The fitted curve was then extrapolated to values at future time slices. The fitting of the curve was then measured using the Forecast RMSE (FRMSE) given by Equation 3-1; -

$$FRMSE = \sqrt{\frac{\sum_{t=1}^T (c_t - r_t)^2}{T}} \quad \text{-----} \quad \text{Eq. 3-1}$$

where T is the number of time steps, c_t is the value of the curve, and r_t is the raw value of the time series at time t . The FRMSE, however, does measure how well the forecast algorithm forecasts future values, in this case, the validation model was used.

3.1.2 The validation model

The validation model was constructed by withholding Nine (9) time steps for validation and fitting the curve to the data that was not excluded. The nine (9) time steps account for 25% of the total thirty-nine (39) time steps at a given location. The forecast values were then compared to the raw values that were withheld using the Validation RMSE (VRMSE) given by Equation 3-2; -

$$VRMSE = \sqrt{\frac{\sum_{t=T-m+1}^T (c_t - r_t)^2}{T}} \quad \text{-----} \quad \text{Eq. 3-2}$$

where T is the number of time steps, m is the number of time steps withheld for validation, c_t is the value forecasted from the first $T-m$ time steps, and r_t is the raw value of the time series withheld for validation at time t .

3.2 Geostatistical Forecast algorithms

3.2.1 Random Forest-based forecasting.

Based Random Forest-based forecasting is based on the random forest algorithm (Cutler & Cutler, 2012). The random forest forecast model was trained with repeated training data at every location of the time series cube. Multiple sets of explanatory and dependent variables were created within a single time series at a location by constructing time windows. In this, the time steps in each window were used as explanatory variables and the next time step was used as an independent variable as shown in **Erreur ! Source du renvoi introuvable.**.. Implying, given the total thirty-nine (39)-year time step of wet and dry conditions, thirty-eight (38) sets of explanatory variables and one (1) dependent variable were used to train the forest at each location.

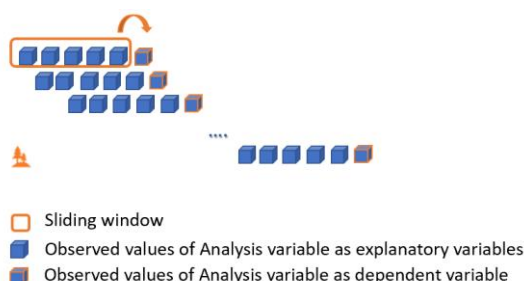


Figure 3: Forest Forecast trained using time windows

Based on the trained forecast model, the final steps of the location are used as an explanatory variable to forecast the first future time step. The second future time step was then forecasted using the

previous time steps in the time window, where one of these time steps is the first forecasted value. This process continues through all future time steps as shown in Figure 4.

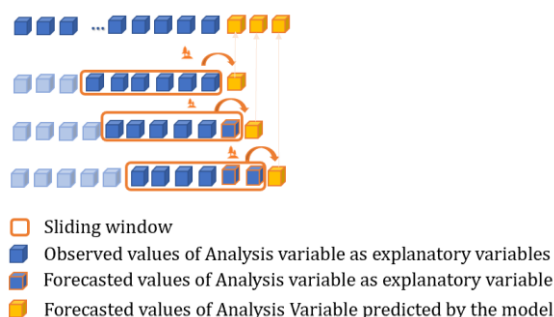


Figure 4: Forecasts are created using time windows

3.2.2 Exponential Smoothing

Exponential smoothing approaches have been around since the 1950s, however, no well-developed models were incorporated with spatial stochastic models for likelihood and prediction combinations (Hyndman et al., 2008). In this approach, forecasts are weighted combinations of past observations with recent observations given more weight than older observations. The algorithm assigns exponentially decreasing weights as observations get older (Kalekar, 2004). In this research, the time series was separated into several components. The values of each component were estimated by exponentially weighting the components from previous time steps such that the influence of each time step decreased exponentially going forward in time. Each component was defined recursively through a state-space model approach (Auger-Méthé et al., 2021), and each component depended on all of the other components. The estimation of these parameters was dependent on maximum likelihood estimation (Myung, 2003). All components are additive such that the forecast model is the sum of the individual components. The seasonal component of one year was explored with the Holt-Winters Damped Seasonal method (Kalekar, 2004).

3.2.3 Curve fitting forecast

In this case, a parametric curve was fit to every location in the space-time cube. The forecasting was done by extrapolating the curve to future time steps. The generated curves for this study were either parabolic, linear or exponential. In the linear, the time series at each location were modelled using a straight line. In the Parabolic, the time series at each location were modelled using a parabolic/quadratic curve. In the exponential, the data was modelled using an exponential/geometric curve. This forecast model works in cases where the time series are easily predictable in trend and there is no strong seasonality in the trend.

3.3 Combined and Suitability Assessment

Based on the VRMSE from each of the three algorithms in Section 3.2. The lowest VRMSE was chosen at every location for each year in the projection range. A combined forecast model based on the least VRMSE was then formed. The model was then interchanged to visualize the algorithm with the least VRMSE at each location. Since the algorithms work best under various time series change conditions, this conditional performance of the algorithms was used as the determinant for suitability.

4 Validation

Areas of a 50 km radius were purposively chosen from the different regions in the country. In this, a fishnet was developed, and centroids were extracted at a 5km radius. A total of 2294 pins were generated across the study area as shown in Figure 5. SPI data sets of 2021 and 2022 were acquired and values were extracted for each of these points. Values for these points were also extracted from each of the map models from the location-based prediction algorithms. R-squared (Nag & Ahmad Malik, 2023) comparisons of the actual values and projected values were run for the exact values of Forest-based, Exponential smoothing, Curve fitting and the best VRMSE map models. The R-squared was repeated for the Exponential smoothing and the Forest-based algorithms whilst accounting for the upper and lower values of the 95% confidence interval.

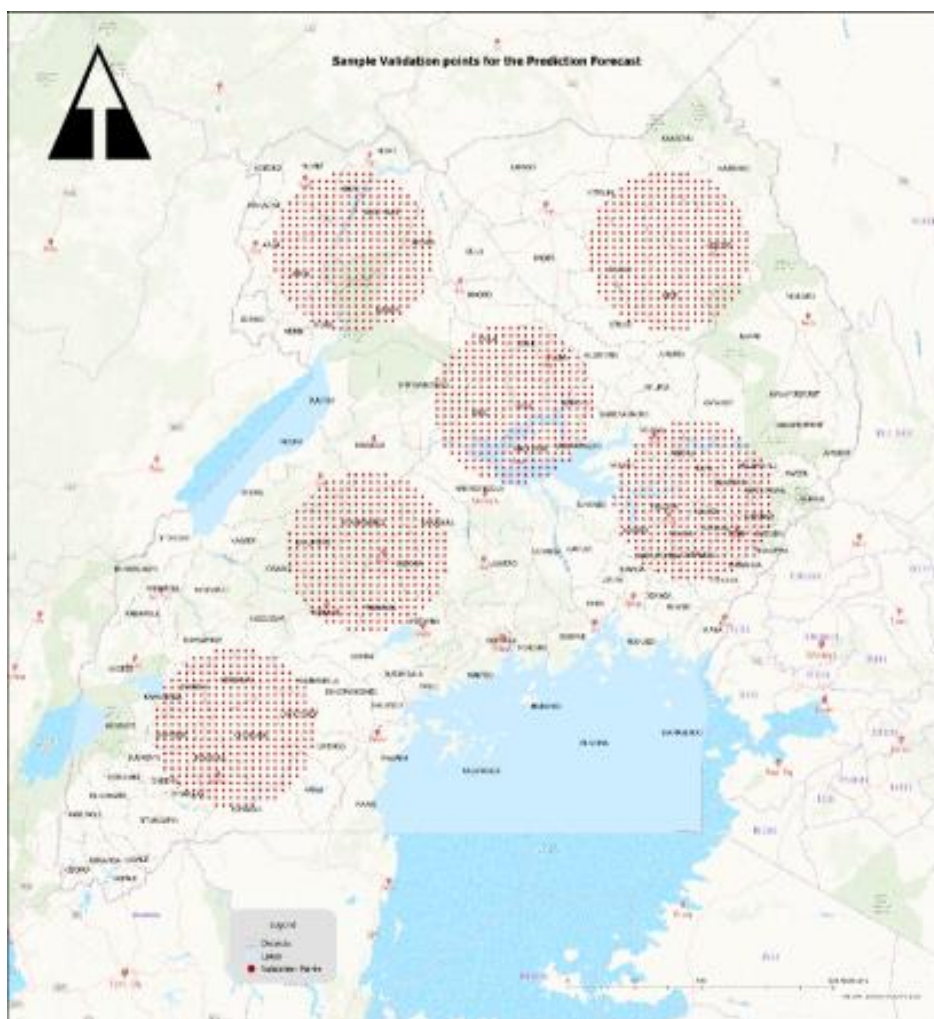


Figure 5: Sample Validation Points

4.1 Results

The location-based forecasting algorithms were able to uniquely produce a time series forecast for every location (cell) within the study area.

4.1.1 Random Forest-based forecasting.

Results from the random forest forecast show that localities within the East and North East parts of the country are likely to experience extremely wet to very wet conditions as indicated in Figure 6.

The districts of Namutumba, Bugiri and Iganga have most of their localities exposed to extreme wet conditions. The northwestern part of Uganda as well as the mid-southwest are characterized by a few localities that will experience dry conditions. Notably, the likely occurrence of extremely wet and very wet conditions is observed in an uneven distribution throughout the country by 2025. The histogram distribution shows that the majority of the localities will be moderately wet to very wet. In the tail ends of the distribution, more areas will experience extreme wet conditions than extreme dry conditions. The trend time series forecast analysis graphs at sampled localities show that the fitted values by the forest forecast algorithm undulate in tandem with the original values. At every time scale, the original value, fitted value and residue can be assessed. The forecast is comprised of a trend line through the different forecast values of the years 2021-2025. The interval between the upper and downward band of the confidence interval takes a convex, increasing with an increase in the time of forecast.

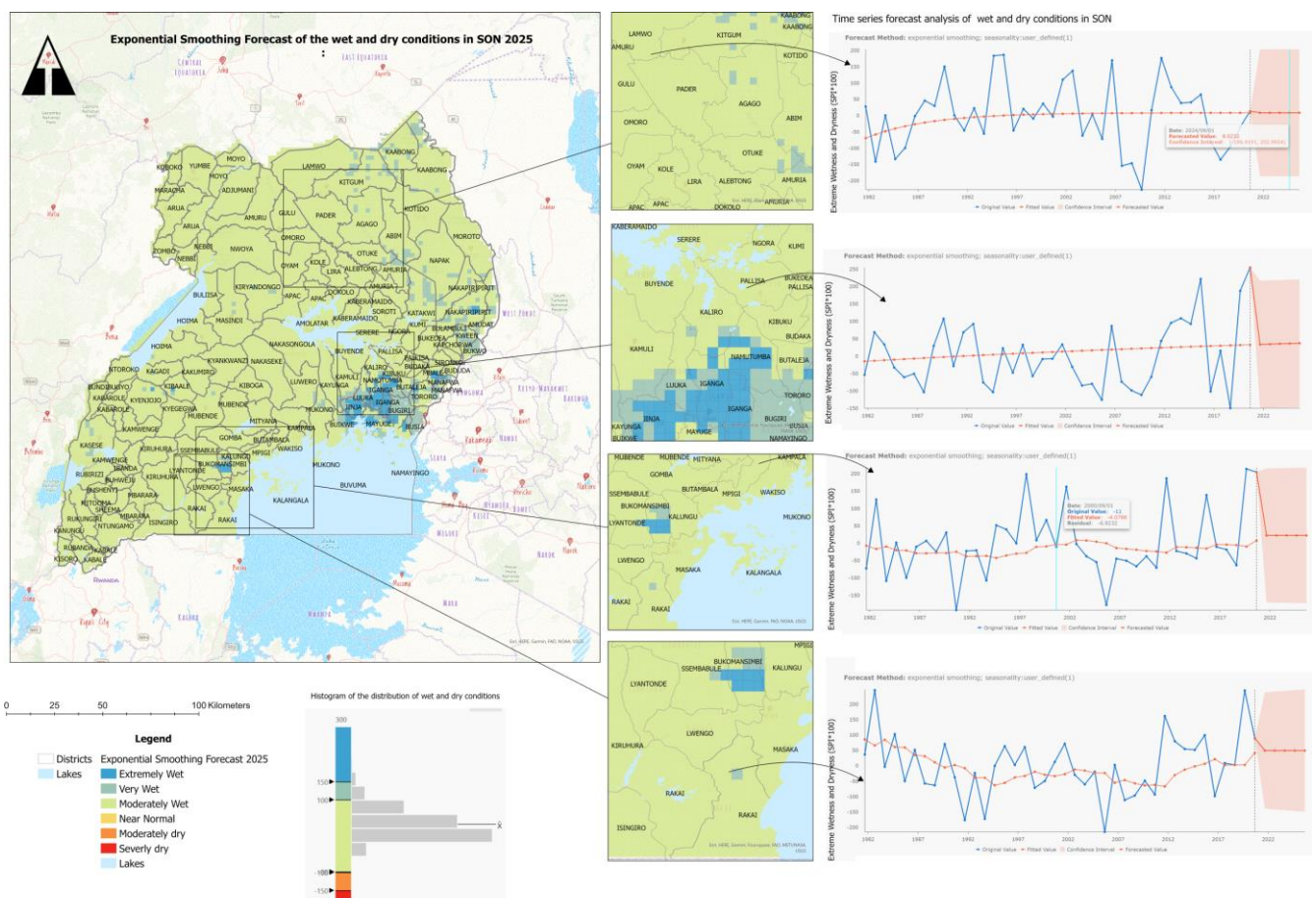


Figure 6: Exponential Smoothing Forecast of Wet and dry conditions in SON 2025

4.1.2 Exponential Smoothing Forecast

Results from the exponential smoothing forecast as shown in Figure7 indicate that a concentration of localities in eastern Uganda, including, Namuntumba, Bugiri, and Iganga will have extremely wet conditions. From the spatial and histogram distribution, most of the areas will experience moderately wet conditions and no dry conditions are projected throughout the study area in the year 2025. The trend time series forecast analysis graphs at sampled locations show that the fitted values by the exponential smoothing mimic the trend of the actual values but do not capture the peaks due to the dumping nature of the algorithm. This accounts for the bigger residue values. The forecast is made of

a trend line and 95% confidence interval band accounting for the upper and lower limits of projection time instance. The band is observed to have an averagely equal upper and lower limit for all the projected values.

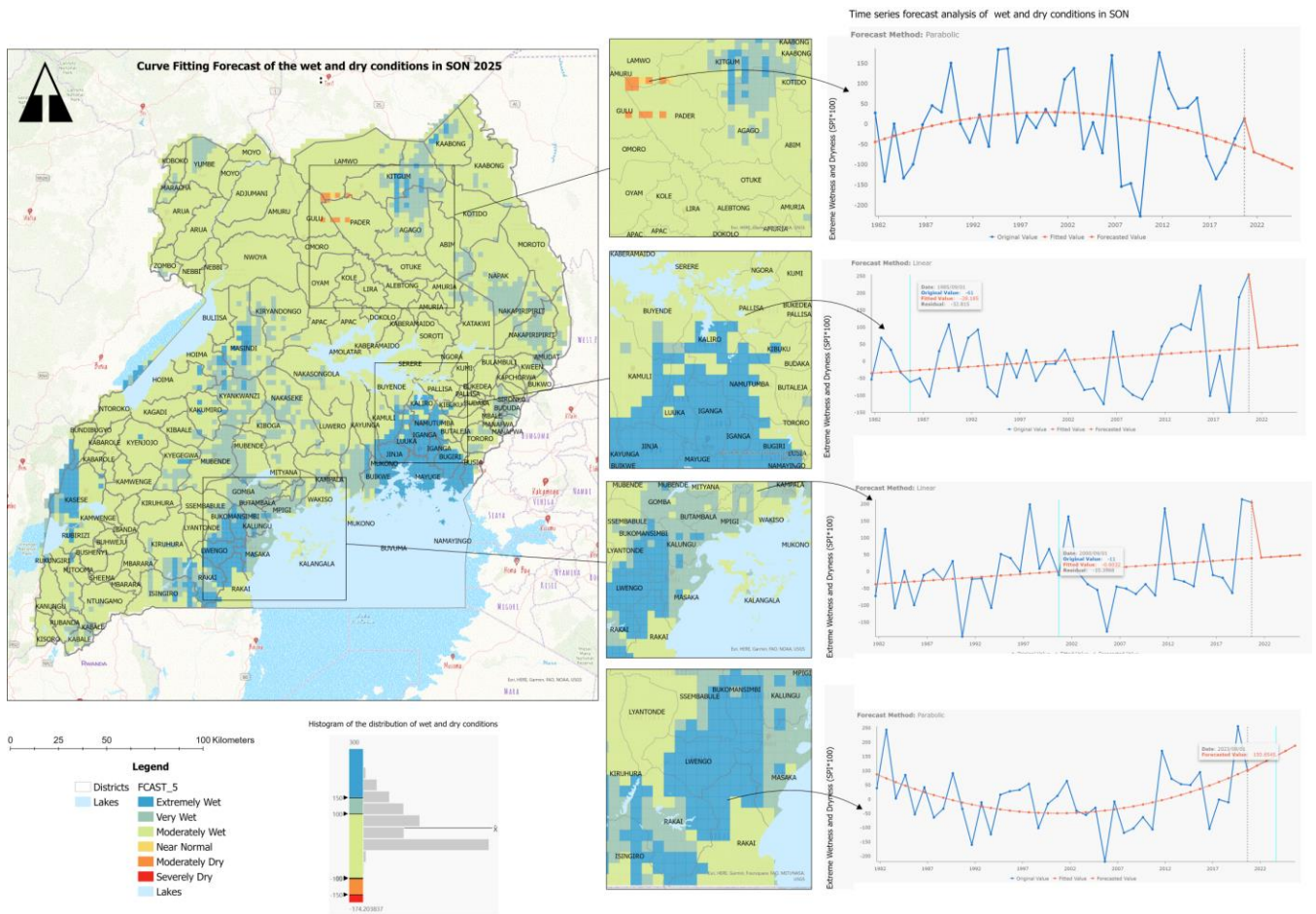


Figure 7: Curve fitting forecast of the wet and dry conditions in SON 2025

4.1.3 Curve fitting forecast

Compared to the exponential smoothing, the curve fitting forecast resultant model for 2025 as shown in **Erreur ! Source du renvoi introuvable.** indicates a wider spread of extremely wet conditions. These are observed in the Middle Eastern part of the country within the districts of Namutumba, Bugiri, Mayuge, Luuka, Iganga, Jinja, Kayunga and Buikwe where several localities are exposed to the likelihood of these extreme wet conditions. Other localities in the south, southwest, and central western Uganda are also observed to have extreme to severe wet conditions by the SON season of 2025. Based on the histogram distribution, the majority of the localities within the country will experience moderately wet conditions. Incidences of dry conditions are observed in some localities in northern Uganda. The trend time series forecast analysis at sampled locations shows that at each locality, a fitting trend curve of either; linear, parabolic or exponential was adopted depending on the trend behaviour of the time series data at that locality.

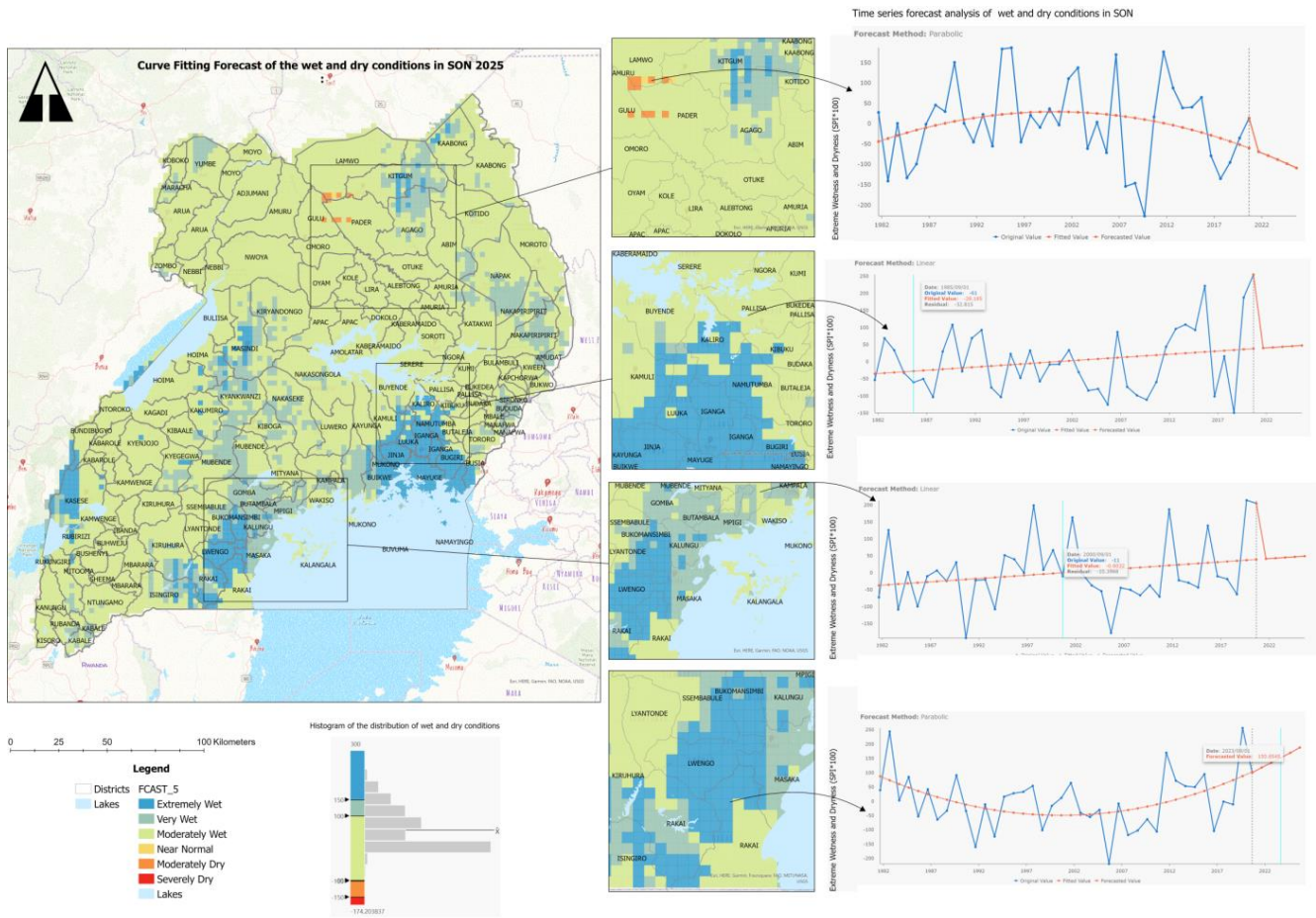


Figure 8: Curve fitting forecast of the wet and dry conditions in SON 2025

4.1.4 Combined Forecast Model

The results of the forest-based, exponential smoothing and curve fitting were combined based on the forecast model with the smallest VRMSE relative to the FRMSE at every locality from each of the algorithms as shown in Figure 9. Results showed that several localities in the Eastern and Southern parts of the country are to experience extreme to very wet conditions. Random localities within the study area show that they will experience near-normal to moderate to severe dry conditions in the same season. In the histogram distribution, the majority of the areas will experience moderately wet conditions with the tail ends of the distribution showing a greater likelihood of extreme wet conditions. The trend time series forecast analysis at every location shows a comparative visualization of trends at every location with the most accurate band highlighted.

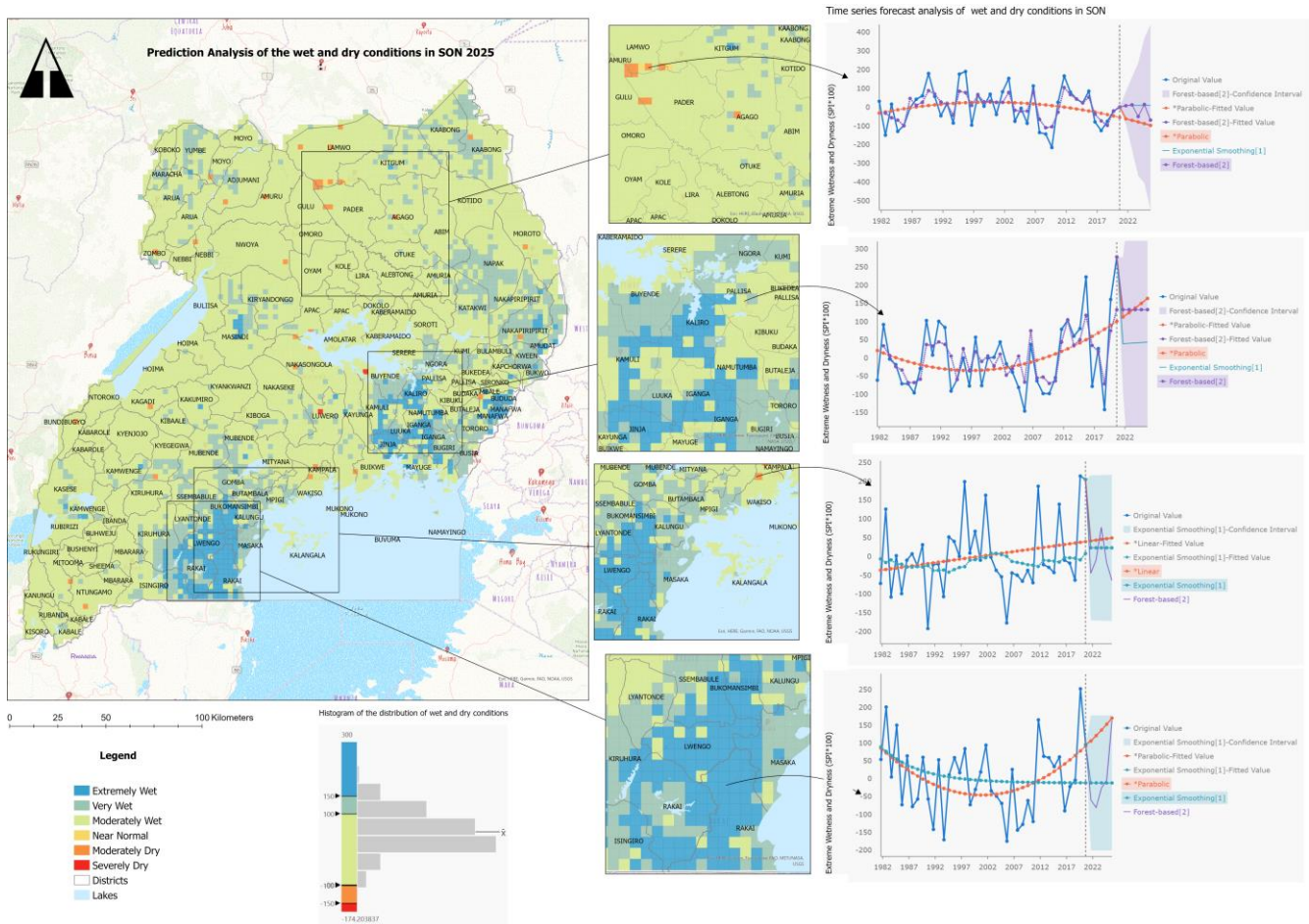


Figure 9: Prediction analysis of the wet and dry conditions in SON 2025

4.1.5 Spatial Suitability of Forecast Algorithm

The combined forecast model was further modified to indicate the least VRMSE not by value but by the contributing forecast algorithm. The resultant model as shown in Figure 10. indicates the algorithms and where they worked best spatially. The algorithm per location count shows that of the 7836 localities at 5km intervals; the forest-based covered 1991 locations, the parabolic 1685, the mean covered 1575, the linear covered 1300 locations and the exponential smoothing covered 1285.

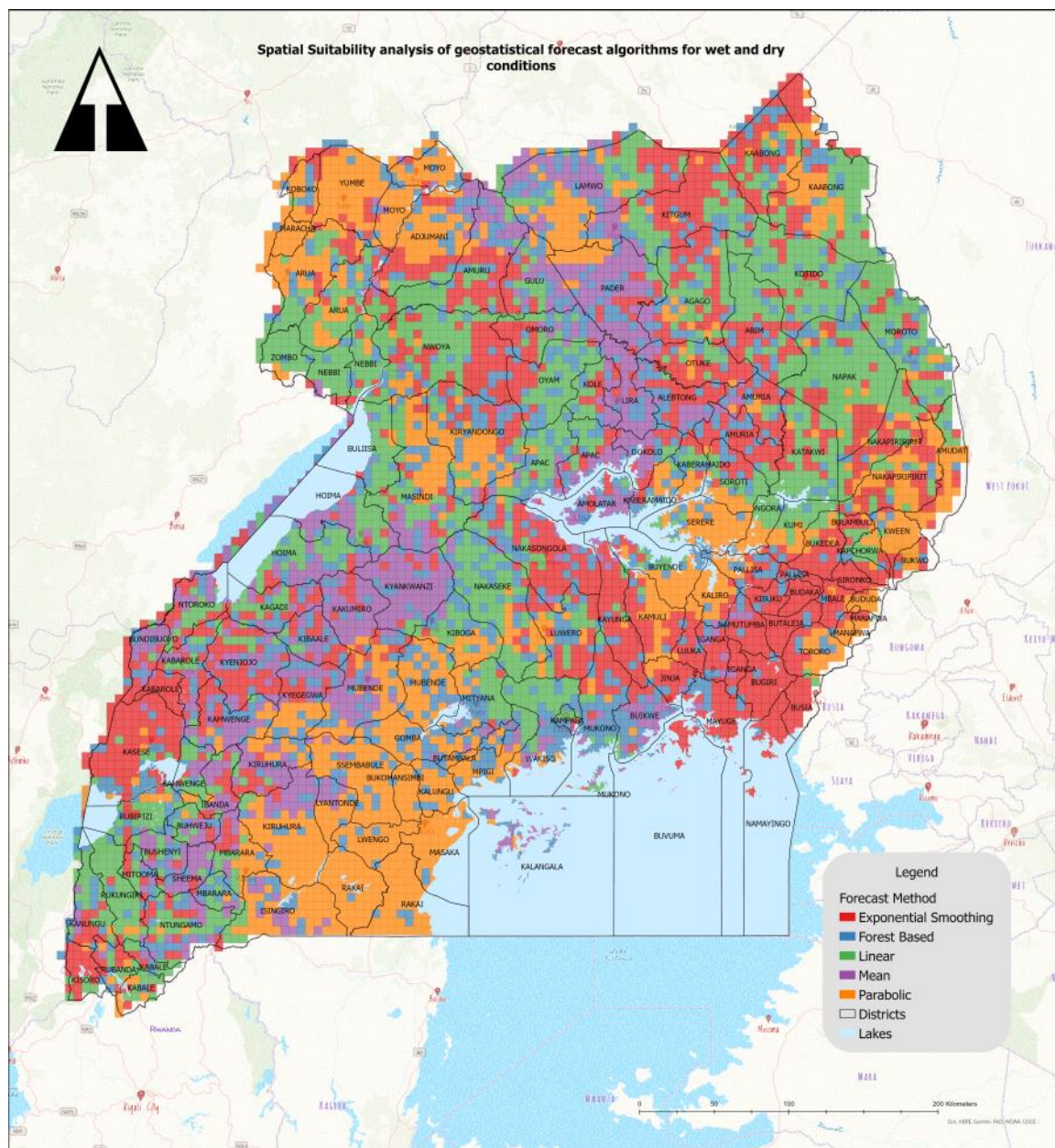


Figure 5: Spatial suitability of wet and dry condition geostatistical forecast algorithms.

4.2 Validation

The validation results as shown in

Table 1 were divided into two parts, those resulting from the comparison of the exact predicted value with the observed value and those that compared the observed value and the values within the confidence interval band. From the exact values, we observe that the forecast algorithms do not perform well in the first year, but improve in the following year with the exception of exponential smoothing. The combination of the algorithms by the least VRMSE gave improved results in the first

year as well as the second year. In the validation of results based on the confidence band, both exponential smoothing and forest-based algorithms performed well.

Table 1: R-squared (R^2) values of the geostatistical forecast algorithms

Year	Exact Value				Inexact (95% Confidence interval)	
	Curve Fitting	Exponential Smoothing	Forest Based	Combined by least VRMSE	Exponential Smoothing	Forest Based
2021	0.27	0.48	0.31	0.58	0.83	0.84
2022	0.40	0.42	0.33	0.62	0.83	0.89

5 Discussion

The histogram observations from Figures 6, Figure 7, Figure 8, and 9, are consistent with observations by Ogwang et al., 2016 that wetter conditions occur in more localities than dry conditions in the SON seasons. The algorithms compared fairly in the spatial distribution of the projections. Using 2025 as the projected year, all the algorithms locate the central-eastern areas of Namutuba, Bugiri, Mayuge, Luuka and Kayunga to have a likelihood of extremely wet conditions, the algorithms indicate a similar behaviour of very wet in the localities on the far east, these areas around the Mountain Elgon region have historically been prone to heavy rains and associated landslides, very wet conditions are also likely in scattered localities in the northeast, lake Victoria region, south of the country, and the far southwest in the mountain Rwenzori region. In all algorithms, most parts of the country experience moderate wet conditions. The location-based algorithm further reveals that the behaviour of wet and dry conditions experienced can be isolated for certain localities.

In the validation of the methods in terms of predicting the exact value, although the proportion of variance (R^2) is below 0.6 for all the algorithms, there is a notice of improvement with longer periods unlike for the exponential smoothing. This is in line with similar studies that noted exponential smoothing to work better in short-term predictions (Hyndman et al., 2008). Although findings by Al-Mistarehi et al., 2022 and Mohapatra et al., 2022 indicate that the Forest algorithm outperforms other machine learning algorithms with the highest accuracy rate measurement, in this case of forecasting, the exact value forecast could not be established with high accuracy. However, in working within the upper and lower limits of the 95% confidence interval, both the exponential smoothing and forest-based algorithms performed well with Forest based algorithm still outperforming the exponential smoothing with longer time forecasts and values within the confidence interval band.

Based on the VRMSE, the forest-based algorithm provided the best value for most areas followed by the parabolic, mean, and linear forecasts in the curve fitting algorithm and then the exponential smoothing. Using the proposition by Zhang et al., 2004, that the characteristics of algorithms available for assessment have an unveiling impact on the nature of the extreme under assessment, the conditional performance of the algorithms was used as a proxy for spatial suitability. The Forest

best algorithm is known to work best in complex trends, exhibiting; up, levelled, and downshift behaviour in a non-systematic manner. This indicatively aligns with the case of many localities in the study region as described in a study by Mubiru et al., 2012 that characterized precipitation across many localities in the country as highly unreliable and erratic in terms of the onset, cessation, intensity, and spatial pattern. The Parabolic is effective in areas where the changes in trend over time either increase or decrease. The linear corresponds to areas where the trend increases and decreases steadily with time. The exponential model is most effective for localities where the trend changes gradually and follows consistent seasonal patterns over time.

6 Conclusion

This study assessed three forecast algorithms: forest-based, exponential smoothing and curve fitting in forecasting wet and dry conditions at a local scale in Uganda. The CHIRPS satellite gridded datasets for the variable short rains season of September, October, and November (SON) for the 1981-2020 historical period were used to develop the forecasts and the 2021-2022 period was used to validate the forecasts. The Standardized Precipitation Index (SPI) was used as the proxy for wet and dry conditions. The three algorithms were assessed by subjecting them to the space-time cube structure, a combination of the CHIRPS-derived SPI values into a NetCDF file based on the 1981-2020 time series. Using the resultant FRMSE and VRSME, forecast models were then generated for each of the three algorithms. A comparison of the least VRSME at every locality from any of the three algorithms was then used to build a joint forecast model.

Results from the three algorithms showed that irrespective of the neighbourhood influence, each locality experiences an independent forecast and by 2025, the majority of the localities will experience moderately wet conditions in the SON. In the three algorithms localities in the middle east have are high likelihood of experiencing extreme wet conditions by 2025. However, the spread of the wet and dry conditions differs from one algorithm to the other. With the exception of exponential smoothing, the other algorithms show a likelihood of dry conditions within certain localities.

The forest-based forecast, exponential smoothing, curve fitting and the combined least VRMSE forecast produced a best value of $R^2=0.33, 0.48, 0.4$ and 0.62 respectively upon validation of the exact value. However, for values within the 95% confidence interval band an $R^2=0.89, 0.83$ was realized for the forest-based and exponential smoothing. Based on the behavioural performance of the algorithms, results further reveal that 25% of the localities in the study area exhibit complex patterns and can best be predicted by Forest based algorithms, 22% of the localities change pattern direction over time and are best predicted by parabolic distributions, 20% of the localities change steadily in one direction and are best predicted by linear forecasts, 17% of the localities have a mean pattern and are best forecast by mean forecasting, 16% have a pattern that's gradually changing but consistent and these are best forecast by exponential smoothing. The results from this study support the motive of the Sustainable Development Goal (SDG) 13 by enabling the communication of empirical studies on locally determined climate contributions. This information derived about wet and dry conditions at a local scale will aid in building the capacity of local governance and decision-making bodies that adopt and implement local disaster risk reduction strategies at a local scale. Further research is needed to assess the driving factors behind the pattern behaviours at the different localities.

7 Acknowledgement

We would like to acknowledge the ESRI Eastern Africa technical support team led by Laban Ndungo for providing continuous support in the development of this research. We also acknowledge the Climate Hazard Center (CHC) for providing the CHIRPS datasets that were used in this study

8 Funding

This research was partly funded by Makerere University.

9 Authors Contributions

Ivan Bamweyana led the research design and execution. Professor Moses Musinguzi and Dr. Lydia Mazzi Kayondo supervised the research, providing control over the structuring, execution and communication of the research objectives

10 References

- Al-Mistarehi, B. W., Alomari, A. H., Imam, R., & Mashaqba, M. (2022). Using Machine Learning Models to Forecast Severity Level of Traffic Crashes by R Studio and ArcGIS. *Frontiers in Built Environment*, 8(April), 1–14. <https://doi.org/10.3389/fbuil.2022.860805>
- Anshuka, A., Chandra, R., Buzacott, A. J. V., Sanderson, D., & van Ogtrop, F. F. (2022). Spatiotemporal hydrological extreme forecasting framework using LSTM deep learning model. *Stochastic Environmental Research and Risk Assessment*, 36(10), 3467–3485. <https://doi.org/10.1007/S00477-022-02204-3>
- Arbia, G., & Di Marcantonio, M. (2015). Forecasting interest rates using geostatistical techniques. *Econometrics*, 3(4), 733–760. <https://doi.org/10.3390/econometrics3040733>
- Atube, F., Malinga, G. M., Nyeko, M., Okello, D. M., Mugonola, B., Omony, G. W., & Okello-Uma, I. (2022). Farmers' perceptions of climate change, long-term variability and trends in rainfall in Apac district, northern Uganda. *CABI Agriculture and Bioscience*, 3(1). <https://doi.org/10.1186/S43170-022-00116-4>
- Auger-Méthé, M., Newman, K., Cole, D., Empacher, F., Gryba, R., King, A. A., Leos-Barajas, V., Mills Flemming, J., Nielsen, A., Petris, G., & Thomas, L. (2021). A guide to state–space modelling of ecological time series. *Ecological Monographs*, 91(4), 1–38. <https://doi.org/10.1002/ecm.1470>
- Bamweyana, I., & Kayondo, L. M. (2017). Spatially Explicit Modelling of Extreme Weather and Climate Events Hot Spots for Cumulative Climate Change in Uganda. *South African Journal of Geomatics*, 7(1). <https://doi.org/10.4314/sajg.v7i1.7>
- Bamweyana, I., Musinguzi, M., Kayondo, L. M. (2021). Evaluation of CHIRPS Satellite Gridded Dataset as an Alternative Rainfall Estimate for Localized Modelling over Uganda. *Atmospheric and Climate Sciences*, 11(4), 797–811. <https://doi.org/10.4236/ACS.2021.114046>
- Chris, F., Jim, R., Gary, E., & Libby, W. (2012). Famine Early Warning Systems Network—Informing Climate Change Adaptation Series A Climate Trend Analysis of Uganda. 1–4.
- Cutler, A., & Cutler, D. R. (2012). Ensemble Machine Learning. *Ensemble Machine Learning*, January. <https://doi.org/10.1007/978-1-4419-9326-7>

- Diem, J. E., Hartter, J., Ryan, S. J., & Palace, M. W. (2014). Validation of satellite rainfall products for Western Uganda. *Journal of Hydrometeorology*, 15(5), 2030–2038.
<https://doi.org/10.1175/JHM-D-13-0193.1>
- Dinku, T., Funk, C., Peterson, P., Maidment, R., Tadesse, T., Gadain, H., & Ceccato, P. (2018). Validation of the CHIRPS satellite rainfall estimates over eastern Africa. *Quarterly Journal of the Royal Meteorological Society*, 144, 292–312. <https://doi.org/10.1002/QJ.3244>
- Ford, T. W., Chen, L., & Schoof, J. T. (2021). Variability and Transitions in Precipitation Extremes in the Midwest United States. *Journal of Hydrometeorology*, 22(3), 533–545.
<https://doi.org/10.1175/JHM-D-20-0216.1>
- Hepworth, N., & Goulden, M. (2008). Climate Change in Uganda: Understanding the implications and appraising the response. *Proceedings of the Institution of Civil Engineers - Energy*, 161(July), 1–48. <https://doi.org/10.1680/ener.2008.161.2.87>
- Hyndman, R. J., Koehler, A. B., Ord, J. K., & Snyder, R. D. (2008). *Springer Series in Statistics Forecasting with Exponential Smoothing*. 350.
https://books.google.com/books/about/Forecasting_with_Exponential_Smoothing.html?id=GSyzox8Lu9YC
- Kalekar, P. S. (2004). *Time series Forecasting using Holt-Winters Exponential Smoothing*. Kanwal Rekhi School of Information Technology
- Khandu, Forootan, E., Schumacher, M., Awange, J. L., & Müller Schmied, H. (2016). Exploring the influence of precipitation extremes and human water use on total water storage (TWS) changes in the Ganges-Brahmaputra-Meghna River Basin. *Water Resources Research*, 52(3), 2240–2258. <https://doi.org/10.1002/2015WR018113>
- Kleiber, W., Raftery, A. E., & Gneiting, T. (2011). Geostatistical model averaging for locally calibrated probabilistic quantitative precipitation forecasting. *Journal of the American Statistical Association*, 106(496), 1291–1303. <https://doi.org/10.1198/jasa.2011.ap10433>
- Kolstad, E. W., & MacLeod, D. (2022). Lagged oceanic effects on the East African short rains. *Climate Dynamics*, 59(3–4), 1043–1056. <https://doi.org/10.1007/S00382-022-06176-6>
- Long, D., Scanlon, B. R., Fernando, D. N., Meng, L., & Quiring, S. M. (2012). Are Temperature and Precipitation Extremes Increasing over the U.S. High Plains? *Earth Interactions*, 16(16), 1–20.
<https://doi.org/10.1175/2012EI000454.1>
- Mohapatra, S., Kundu, M., & Mohanty, S. (2022). Climate Downscaling and Prediction Using GIS-Based Machine Learning. *2022 2nd International Conference on Computer Science, Engineering and Applications, ICCSEA 2022*.
<https://doi.org/10.1109/ICCSEA54677.2022.9936384>
- Mubiru, D. N., Komutunga, E., Agona, A., Apok, A., & Ngara, T. (2012). Characterising agrometeorological climate risks and uncertainties: Crop production in Uganda. *South African Journal of Science*, 108(3–4). <https://doi.org/10.4102/sajs.v108i3/4.470>
- Mugenyi, O., Kaggwa, R., Kisaame, K. E., & Solomon, S. (2011). MARGINALIZATION OF

ENVIRONMENT AND NATURAL RESOURCES SUB-SECTOR Undermining the Economic Base and Entrenching Poverty in Uganda. 24, 1–26.

Muthoni, F. K., Odongo, V. O., Ochieng, J., Mugalavai, E. M., Mourice, S. K., Hoesche-Zeledon, I., Mwila, M., & Bekunda, M. (2019). Long-term spatial-temporal trends and variability of rainfall over Eastern and Southern Africa. *Theoretical and Applied Climatology*, 137(3–4), 1869–1882. <https://doi.org/10.1007/S00704-018-2712-1/FIGURES/10>

MWLE, GEF, U. (2002). Initial National Communication of Uganda to the Conference of the Parties to the United Nations Framework Convention on Climate Change.

Myung, I. J. (2003). Tutorial on maximum likelihood estimation. *Journal of Mathematical Psychology*, 47(1), 90–100. [https://doi.org/10.1016/S0022-2496\(02\)00028-7](https://doi.org/10.1016/S0022-2496(02)00028-7)

Nag, M. B., & Ahmad Malik, F. (2023). Data Analysis and Interpretation. *Repatriation Management and Competency Transfer in a Culturally Dynamic World*, 93–140. https://doi.org/10.1007/978-981-19-7350-5_5

Ngoma, H., Wang, W. A., Ayugi, B., Karim, R., Kisesa Makula, E., Wen, W., & Makula, K. (2021). Mechanisms associated with September to November (SON) rainfall over Uganda during the recent decades. *Geographica Pannonica* •, 25(1), 10–23. <https://doi.org/10.5937/gp25-29932>

Nsubuga, F. W., & Rautenbach, H. (2018). Climate change and variability: a review of what is known and ought to be known for Uganda. *International Journal of Climate Change Strategies and Management*, 10(5), 752–771. <https://doi.org/10.1108/IJCCSM-04-2017-0090>

Ogwang, B. A., Ayesiga, G., Ojara, M., Kalema, A., Nimusiima, A., Tindamanyire, T., Serwanga, M. N., Ssebabi, F., Gugwa, G., Nsubuga, Y., Atim, R., Kibwika, R., Kiwuwa Balikudembe, J., Kikonyogo, H., Ongoma, V., Taire, A., Kiryhabwe, A., Semujju, M., Einyu, F., ... Kituusa, R. (2016). Characteristics and changes in SON rainfall over Uganda (1901-2013). *Journal of Environmental and Agricultural Sciences*, 8(September 2018), 45–53. <https://www.researchgate.net/publication/306324232>

Osbahr, H., Dorward, P., Stern, R., & Cooper, S. (2011). Supporting agricultural innovation in Uganda to respond to climate risk: Linking climate change and variability with farmer perceptions. *Experimental Agriculture*, 47(2), 293–316. <https://doi.org/10.1017/S0014479710000785>

Purwanto, P., Utaya, S., Handoyo, B., Bachri, S., Astuti, I. S., Sastro, K., Utomo, B., & Aldianto, Y. E. (2021). Spatiotemporal analysis of COVID-19 spread with emerging hotspot analysis and space-time cube models in East Java, Indonesia. *ISPRS International Journal of Geo-Information*, 10(3). <https://doi.org/10.3390/ijgi10030133>

Res, C., Vicente-serrano, S. M., Saz-sánchez, M. A., & Cuadrat, J. M. (2003). Comparative analysis of interpolation methods in the middle Ebro Valley (Spain): application to annual precipitation and temperature. 24, 161–180.

SNC. (2014). Uganda Second National Communication to the United Nations Framework Convention on Climate Change. 213.

USAID. (2013). Uganda Climate Change Vulnerability Assessment Report. 0–77.

Wang, R., Chen, J., Chen, X., & Wang, Y. (2017). Variability of precipitation extremes and dryness/wetness over the southeast coastal region of China, 1960–2014. *International Journal of Climatology*, 37(13), 4656–4669. <https://doi.org/10.1002/JOC.5113>

Zhang, X., Canada, E., Li, G., & Canada, E. (2004). Monte Carlo Experiments on the Detection of Trends in Extreme Values. *Journal of Climate*, 0442(May 2004). [https://doi.org/10.1175/1520-0442\(2004\)017<1945](https://doi.org/10.1175/1520-0442(2004)017<1945)

11 KEY TERMS AND DEFINITIONS

Precipitation: A type of water that condenses from the sky and falls to the Earth's surface as rain, snow, or sleet because it is too heavy to stay suspended. In this study rain is the proxy for precipitation

Wet and dry conditions: Wet conditions occur as areas receive high amounts of precipitation resulting in high levels of humidity and frequent rain. While dry conditions occur as a result of less precipitation and lower atmospheric temperature, dry conditions are defined climatically by strong solar radiation.

Local Scale: The spatial extent of 0-10km² within which geographical phenomena such as precipitation can be analysed. In this study spatial units (cells) of 5km² were analysed.

Geostatistics: Refers to measures based on statistical techniques that are deployed to describe and quantify how occurrences, like precipitation, are distributed throughout time and space on Earth, with a focus on the nature of spatial data.

Precipitation Forecasting: Refers to computation and estimation that creates a quantitative and/or qualitative future outcome of precipitation occurrences by using spatial and time series data from historical precipitation records along with current trends.